Applied Surface Science 389 (2016) 278–286

Contents lists available at ScienceDirect

Applied Surface Science

journal homepage: www.elsevier.com/locate/apsusc

Fabrication and characterization of PbO_2 electrode modified with polyvinylidene fluoride (PVDF)

Xiaoliang Li, Hao Xu*, Wei Yan*

Department of Environmental Science and Engineering, State Key Laboratory of Multiphase flow in Power Engineering, Xi'an Jiaotong University, Xi'an 710049, China

ARTICLE INFO

Article history:
Received 20 June 2016
Received in revised form 18 July 2016
Accepted 20 July 2016
Available online 21 July 2016

Keywords:
PbO_2 electrode
PVDF
Modification
Electrocatalytic activity
Stability

ABSTRACT

A novel PbO_2 electrode with a high oxygen evolution potential (OEP) and long service life was successfully fabricated by doping polyvinyl fluoride (PVDF) (marked as PbO_2-PVDF) through co-deposition method. The morphology (SEM), elemental analysis (EDX), hydrophobic property (contact angle), crystalline structure (XRD), chemical state (XPS), electrochemical performances (Lsv and EIS) and stability (accelerated life test) were characterized. The results showed that PVDF doping could improve the film morphology, increase oxygen evolution potential (OEP) and reduce the electrode film impedance. In addition, the proportion of adsorbed hydroxyl oxygen (O_{ad}) on the electrode also increased. During the electrochemical oxidation process, the PbO_2-PVDF(2.0) electrode showed the best performance on degradation of phenol due to the highest removal rate, lowest energy consumption and minimum Pb dissolution, which could be attributed to its hydrophobic surface, high oxygen evolution potential (OEP) and strong capability of $HO^{\bullet}$ generation. Furthermore, the stability of the electrodes were greatly improved after PVDF modification. PbO_2-PVDF(1.0) electrode showed the longest service life (501 h), which was more than 4 times longer than PbO_2 electrode (118.5 h).

© 2016 Published by Elsevier B.V.

1. Introduction

Electrochemical oxidation treatment (EOT), an attractive wastewater treatment technology, has been widely applied in wastewater treatment due to its high efficiency, mild condition, easy operation and environmental friendliness [1,2]. Anode as the core component is particularly important in the electrochemical oxidation process [3,4]. Therefore, it is essential to develop an excellent electrode with high catalytic activity and stability at low cost [5].

So far, various types of electrodes have been investigated. Such as graphite [6], Pt [7], boron-doped diamond (BDD) [8] and dimensionally stable anodes (Ti/IrO_2 [9], Ti/RuO_2 [10], Ti/MnO_2 [11], Ti/SnO_2 [12] and Ti/PbO_2 [13], etc.). Among these electrodes, Ti/PbO_2 was regarded as the most promising electrode and has been successfully used in EOT process due to its high electrocatalytic activity, high chemical stability, ease of synthesis as well as low cost [14–16]. However, due to its relatively large interface resistance, the surface coating would peel off easily, leading to the leakage of Pb elements [5,17]. In addition, the electrocatalytic activity of Ti/PbO_2 electrode is still lower compared with BDD and Ti/SnO_2 electrodes [8,18]. Therefore, the stability and electrocatalytic activity of the Ti/PbO_2 electrode still need further improvement. To solve the problem, many efforts have been devoted, including modifying substrate [19,20], introducing the middle layer [21,22] and doping elements [15,23–25]. Meanwhile, some polymers materials, such as polyvinylpyrrolidone (PVP) [26], Polypyrrole (PPy) [27], fluorine resin [28] and polytetrafluoroethylene (PTFE) [29] were also adopted to enhance the electrochemical oxidation ability and stability of PbO_2 electrode. The results show that the introduction of polymers materials could effectively improve the properties of PbO_2 electrode.

Polyvinyl fluoride (PVDF) is an important and excellent polymer, possessing many excellent properties such as excellent chemical corrosion resistance, flexibility, high abrasion resistance, hydrophobicity and low cost, which has been extensively investigated and applied in many industrial fields [30–32]. Therefore, the PbO_2 electrode modified with PVDF may be promising and interesting. However, the study of electrodes modified with PVDF is rarely reported. Zhao et al. [5] has prepared a hydrophobic PbO_2 electrode with high OEP and excellent electrochemical oxidation performance by doping with fluorine resin. The literature points out that the electrode with a hydrophobic surface is more favorable for improving the utilization rate of $HO^{\bullet}$ radical. In

* Corresponding authors.
E-mail addresses: xuhao@xjtu.edu.cn (H. Xu), yanwei@xjtu.edu.cn (W. Yan).

http://dx.doi.org/10.1016/j.apsusc.2016.07.123
0169-4332/© 2016 Published by Elsevier B.V.

addition, F doping could greatly enhance the service life of PbO_2 electrode.

Therefore, in this work, PVDF composite doped PbO_2 electrode was successfully developed to form a hydrophobic PbO_2-PVDF electrode with excellent electrocatalytic activity and stability. The morphology, hydrophobic property, crystalline structure, chemical state, electrochemical performances and stability were characterized. The capability of HO• generation on the electrodes were also evaluated. One of the widely used crude material, phenol, was chosen as the model pollutant for electrochemical oxidation in order to evaluate its electrochemical ability. Besides, Pb element leaching of PbO_2 electrodes was also studied during electrolysis process to evaluate the safety.

2. Experimental

2.1. Chemicals and reagents

All chemicals used in experiment were obtained from Sinopharm Chemical Reagent Xi'an Co., Ltd and were of analytical grade without further purification. The aqueous solutions were deionized water (18 MΩ cm). PVDF composite (size 6.5 μm, French arkoma HSV900) were purchased from Shanghai Shi Quan Industrial Co., Ltd.

2.2. Electrode preparation

Ti plates (Purity >99.6%, BaoTi Ltd., China) with a dimension of 3 cm × 3 cm × 0.5 mm were used as the electrode substrate. The pre-treatment of Ti plate and introduction of inner Sb–SnO_2 layer were the same as our previous work [15,23]. The surface PbO_2-PVDF layer was coated on the Ti/Sb–SnO_2 electrode through the electrochemical deposition process. In this step, 100 mL solution contained 0.5 mol L^{-1} $Pb(NO_3)_2$, 0.1 mol L^{-1} $Cu(NO_3)_2$, 0.01 mol L^{-1} NaF, 5 mL *N*-methyl pyrrolidone (DNP), 0.1 mol L^{-1} HNO_3 and certain amounts of PVDF composite (0 g L^{-1}, 0.1 g L^{-1}, 0.25 g L^{-1}, 0.5 g L^{-1}, 1.0 g L^{-1} and 2.0 g L^{-1}) was adopted as the deposition solution (marked as PbO_2, PbO_2-PVDF(0.1), PbO_2-PVDF(0.25), PbO_2-PVDF(0.5), PbO_2-PVDF(1.0), and PbO_2-PVDF(2.0), respectively). Finally, the mixed solution stirred for 1 h in the ultrasonic environment for use. The electrochemical deposition processes were performed at 65 °C for 120 min under the anodic current density of 10 mA cm^{-1}. Two copper sheets was used as the counter electrode. Finally, the electrodes were rinsed with deionized water and dried in the oven. The average amount of PbO_2-PVDF surface coating of all electrode are 92 ± 0.7 mg cm^{-2}.

2.3. Characterization analysis

2.3.1. Physicochemical characterizations

Scanning electron microscopy (SEM, JEOL, JSM-6390A) equipped with an energy-dispersive X-ray analyzer (EDX) were used to observe the morphology and elemental analysis. X-ray diffraction (XRD, PAN alytical, Holland) using Cu Kα source (λ = 0.15416 nm) was adopted to analyze crystal structure. The scanning angle (2θ) ranges from 10° to 80°. The contact angle meter (Attension, Theta, Biolin Scientific) was employed to investigate the contact angle of water on the electrode surface.The chemical states of the coatings were studied using the X-ray photoelectron spectroscopy (XPS) (UK; Al Kα radiation, 150 W, 15 kV and 1486.6 eV). The C 1s peak (284.8 eV) was used to calibrate the binding energies. During the process of electrolysis, the concentration of Pb element in the electrolyte was monitored by inductively coupled plasma atomic emission spectroscopy (ICP-AES, ICPE-9000, Shimadzu, Japan).

2.3.2. Electrochemical characterizations

The electrochemical measurements were performed at an electrochemical workstation (CHI 660D, Chenhua, Shanghai, China) in a three electrode cell system. Copper sheets were acted as the counter electrode and Ag/AgCl (sat KCl) was acted as reference electrode. The measure of linear sweep voltammograms (Lsv) was performed in 0.5 mol L^{-1} Na_2SO_4 solution at the scan rate of 0.05 V s^{-1} from 0 V to 2.5 V. EIS measurements were also performed in 0.5 mol L^{-1} Na_2SO_4 solution. The measurement potential was 0 V and the frequencies swept from 10^5 Hz to 0.1 Hz with an sine wave of 5 mV amplitude.

The accelerated lifetime test was performed at an electrochemical workstation (LK3000A, Tianjin Lanlike, China). The selected electrodes were tested at the anode current density of 500 mA cm^{-2} under 35 °C ± 2 °C and the electrolyte was 3 mol L^{-1} H_2SO_4 solution. When the cell voltage raised to 10 V, the selected electrodes was considered to be deactivation.

2.4. Electrochemical oxidation process

Electrochemical oxidation of phenol was carried out in a glass beaker equipped with a magnetic stirrer. The working anodes (PbO_2-PVDF) with an area of 18 cm^2 was used as the anode and copper sheet with the same area was used as the cathode. The distance between the electrodes was 1 cm. The volume of phenol solution was 200 mL and the initial phenol concentration was 100 mg L^{-1}. In order to maintain the conductivity of the solution, 0.1 mol L^{-1} Na_2SO_4 was added to the aqueous solution. Experiments were carried out at room temperature for 5 h at current density of 50 mA cm^{-2}. The samples were monitored and analyzed every 1 h. The concentrations of phenol were quantified by high performance liquid chromatography (HPLC, Dalian Elite Analytical Instruments Co.,Ltd) using an ACE 5 C18 column (250 × 4.6 mm). 60% methanol: 40% water (v:v) was acted as the mobile phase, and the flow rate of the mobile phases was 1.0 mL min^{-1}. The temperature of the columns was 30 °C and the UV–vis detector was set at 270 nm. 20 μm samples were injected to the HPLC. COD reactor (ET 125 SC, CSB/COD Reactor) was used to determine the value of chemical oxygen demand (COD). Besides, instantaneous current efficiency (ICE) and energy consumption (E_p, kWh·gCOD^{-1}) were also be calculated as follows:

$$ICE = \frac{\left(COD_{t_1} - COD_{t_2}\right)}{8I(t_1 - t_2)}FV \quad (1)$$

$$E_p = \frac{UIt}{(COD_{t_1} - COD_{t_2})V} \quad (2)$$

Where and are the values of COD at times t_1 and t_2, respectively, F is the Faraday constant (96,487 C mol^{-1}), I is the current (A), t is the electrolysis time (h), U is the cell voltage (V) and V is the volume of the electrolyte (L).

In order to compare the ability for HO• generated by the electrodes. The concentration of HO• after electrolysis for 0.5 h and 1 h are determined with dimethyl sulfoxide (DMSO) trapping and high-performance liquid chromatography (HPLC, Dalian Elite Analytical Instruments Co.,Ltd) according to literature [33]. The details are shown in S1 of the Supporting information.

3. Results and discussion

3.1. Surface morphology and hydrophobic property of the electrodes

Fig. 1 shows the SEM images of the PbO_2 electrodes prepared with different PVDF doping amounts. From Fig. 1a, it could be observed that the PbO_2 electrode was rough with typical pyramidal

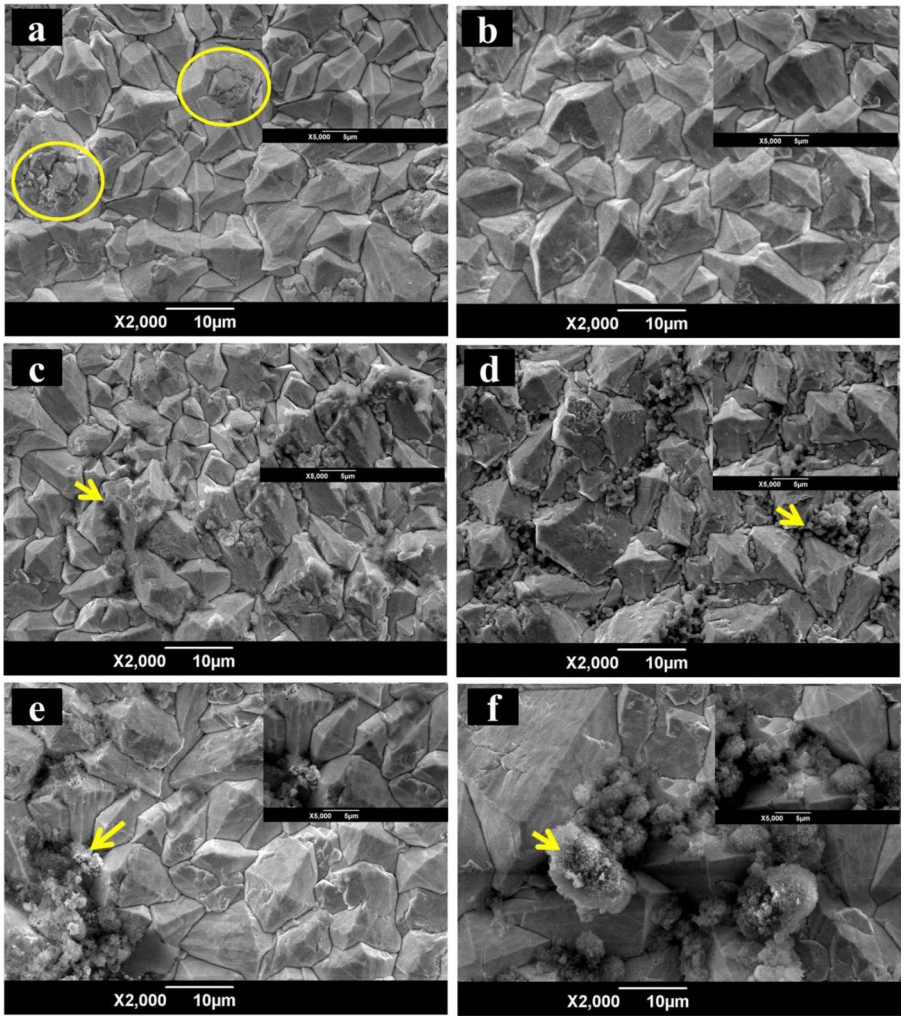

Fig. 1. SEM images of the different PbO_2-PVDF electrodes (a: PbO_2, b: PbO_2-PVDF(0.1), c: PbO_2-PVDF(0.25), d: PbO_2-PVDF(0.5), e: PbO_2-PVDF(1.0), f: PbO_2-PVDF(2.0)).

shapes on the surface [23]. After further observation, some damages and cracks were found on the surface (Inside the circle). This morphology could cause the decrease of the stability of the electrodes in the electrolysis, because electrolyte may permeate the Ti substrate through the damages and cracks easily, forming high-resistance TiO_2 layer and leading to deactivation of electrode [5,19]. Fig. 2b–f shows the microstructures of PbO_2 electrode doped with different PVDF amounts from less to more. After the introduction of PVDF into PbO_2 film, it could be seen that the surface of PbO_2-PVDF electrodes were more integrated and the cracks on PbO_2 electrodes surface disappeared. This result indicated that introducing PVDF into the coating was favorable to decrease cracks on the coating surface and improve the film morphology. In addition, with the increase of doping amount of PVDF, some unidentified particles appeared on the surface of the electrodes (Arrow position of Fig. 2c–f). After EDX test, these particles were proved to be PVDF composites (Fig. S1), proving that the PVDF composites were successfully doped into the PbO_2 electrode.

Fig. 2 shows the contact angles of PbO_2 electrodes with different PVDF doping amounts. The contact angle is an important measure of the relationship between the reaction substance and the liquid wetting property. From Fig. 2a, it could be observed that the contact angles of pure PbO_2 electrode was 62.5°. With the increase of PVDF doping amount, the contact angle increased from 79.2° to 125.5°, indicating that the hydrophobicity of the electrode surface has been improved obviously due to the hydrophobic property of PVDF. Therefore, the enhancement of hydrophobicity and the doping of F element indicated that the catalytic activity and stability of the electrode could be improved effectively according to the literature [5]. Further validation was carried as follows.

3.2. EDX spectrums and elemental mappings

Fig. 3 shows the EDX spectrums and elemental mappings of different PbO_2 electrodes (EDX spectrum of pure PbO_2 electrode is shown in Fig. S2 and no C, F element are detected). From EDX spectrums, it could be seen that the elements of C, O, Pb and F were detected by EDX on PbO_2-PVDF electrodes. In addition, with the increase of PVDF doping amount, the content of C and F elements were gradually increased from 26.53%, 3.18% to 31.57%, 7.08% (atom%). From elemental mapping, it could be also seen that the elements of C and F were uniformly distributed on the surface coating and the densities increased with the increase of PVDF doping amount. From the above results, it was proved that the PVDF composite were successfully and evenly doped into PbO_2 electrodes. Furthermore, no Ti, Sn and Sb elements were detected, indicating that the electrodes surface were covered completely by PbO_2 layer.

3.3. Structure of PbO_2-PVDF electrodes

The XRD patterns of the PbO_2-PVDF electrodes are shown in Fig. 4. From the figure, it could be observed that the main diffraction peaks of the PbO_2 electrode at 25.4°, 32.0°, 36.2° and 49.0°

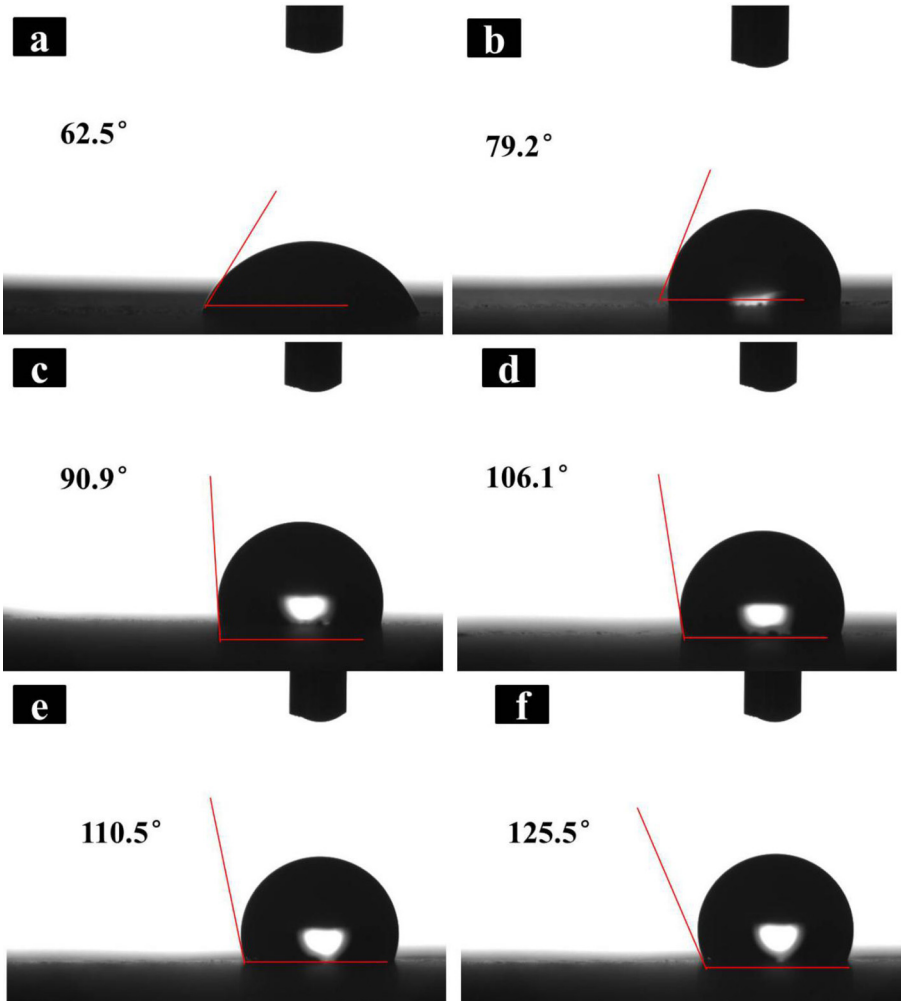

Fig. 2. Contact angles of the different PbO_2-PVDF electrodes (a: PbO_2, b: PbO_2-PVDF(0.1), c: PbO_2-PVDF(0.25), d: PbO_2-PVDF(0.5), e: PbO_2-PVDF(1.0), f: PbO_2-PVDF(2.0)).

were assigned to the (110), (101), (200) and (211) plane of β-PbO_2, respectively. After PVDF doping, the peaks of PVDF at 19.9° are detected contrasting with the XRD pattern of PVDF composites in Fig. S3. In addition, it could be seen that with the increase of doping amount of PVDF, the peaks intensity of PVDF were enhanced, indicating that the doping amount of PVDF increased in the PbO_2 surface layer. When PVDF was doped into the PbO_2 electrode, the crystalline orientation was unchanged. However, the main peaks intensity of PbO_2-PVDF electrodes was lower than that of PbO_2 electrode indicating that the PVDF doping may affect the crystal growth of the PbO_2 electrode. For another reason, the partial PVDF composites had covered the PbO_2 surface, leading to a decrease in the intensity of PbO_2 diffraction peak. Furthermore, from the XRD patterns, it could not seen the peaks of SnO_2, Sb_2O_3 and Ti, indicating the PbO_2 coating had the better coverage of the Sb-SnO_2 interlayer and Ti substrate.

3.4. Linear sweep voltammograms (Lsv) and electrochemical impedance spectroscopy (EIS)

Fig. 5 shows the linear sweep voltammograms (Lsv) of the PbO_2-PVDF electrodes in 0.5 mol L^{-1} Na_2SO_4 solution. As shown in Fig. 5 and Table S2, it could be seen that with the increase of PVDF doping amount, the oxygen evolution potential (OEP) of the modified PbO_2 electrodes were enhance and increased from 1.845 V (PbO_2 electrode) to 1.927 V (PbO_2-PVDF(2.0) electrode). This result indicated that the OEP of PbO_2-PVDF(2.0) electrode was 82 mV higher than that of PbO_2 electrode. It was generally known that an anode with a high OEP was desirable due to the inhabitation of unwanted power loss on oxygen generation [34,35]. Therefore, the higher OEP of PbO_2-PVDF(2.0) electrode indicated that a higher catalytic activity would be exhibited for pollutants degradation. The reason for OEP enhancement could be explained as that with the addition of PVDF composites, the hydrophobicity of the electrodes were improved and inhibited the surface adsorption of hydrophilic $HO^{\bullet}$. Meanwhile, PVDF composites could also restrain the movement and expansion of the free oxygen atoms to the electrode interior and increase the free $HO^{\bullet}$, so that the reaction for O_2 evolution was inhibited [5].

Fig. 6 shows the Nyquist plots of freshly prepared PbO_2-PVDF electrodes in 0.5 mol L^{-1} Na_2SO_4 solutions and the corresponding simulated data are shown in Table S3. The EIS data of all tested electrodes fit the equivalent circuit $R_s(R_fQ)$ very well (solution resistance (R_s), electrode film resistance (R_f) and the constant phase element (Q)). Qualitatively, it could be observed that with the PVDF doping amount from less to more, the arc diameter decreased. As shown in Table S3, it could be obviously seen that the R_f value decreased from 48.1 Ω cm^{-2} (PbO_2 electrode) to 33.62 Ω cm^{-2} (PbO_2-PVDF(2.0) electrode), which indicated that the PVDF composites modification could decrease electrode impedance and favor electron transfer effectively. Moreover, the PbO_2-PVDF(2.0) electrode showed the highest capacitance, implying that more electrochemically active sites would exist on the surface area of electrode coatings [36].

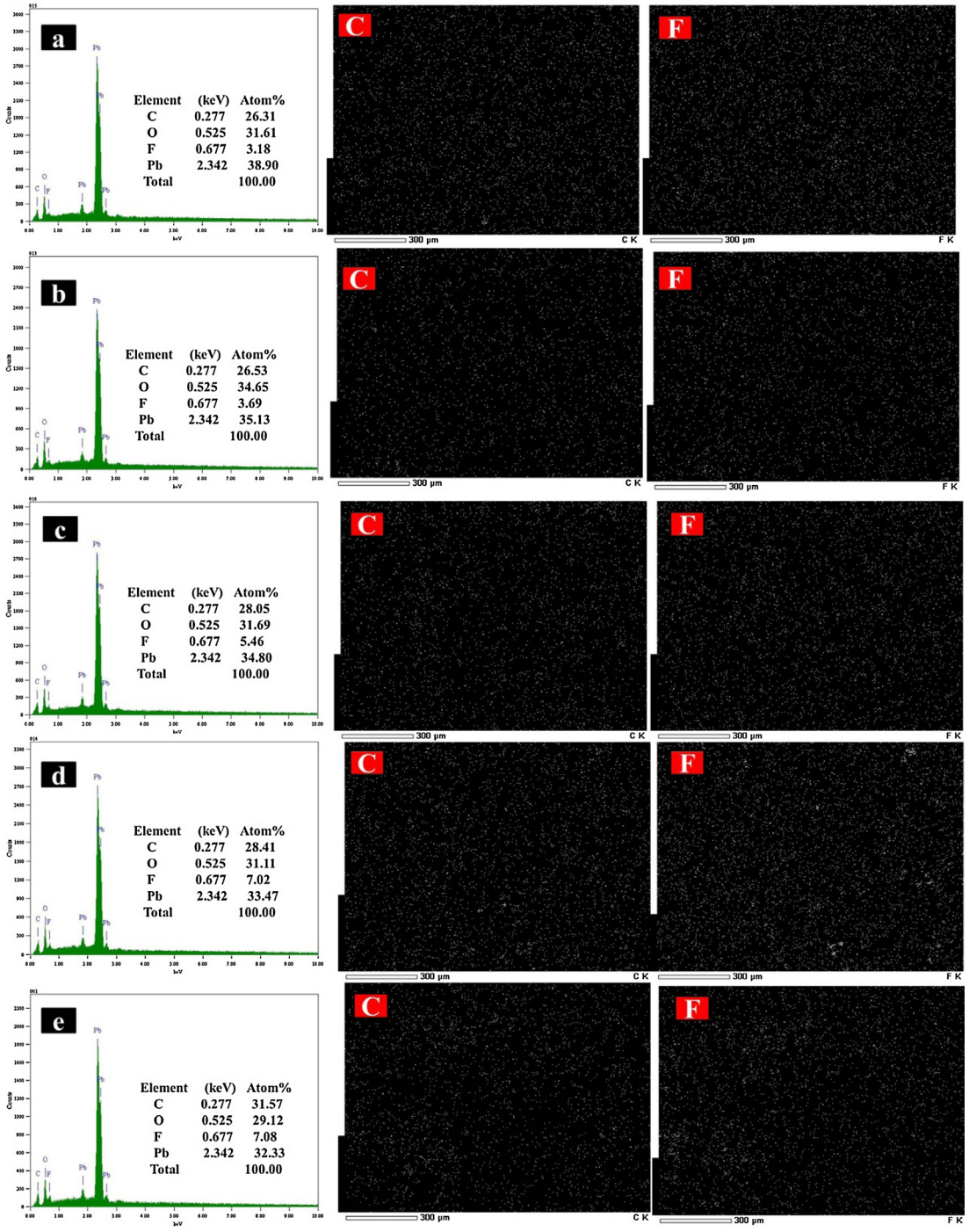

Fig. 3. EDX spectrum and the EDX elemental mapping of C, F of the different PbO_2-PVDF electrodes (a: PbO_2-PVDF(0.1), b: PbO_2-PVDF(0.25), c: PbO_2-PVDF(0.5), d: PbO_2-PVDF(1.0), e: PbO_2-PVDF(2.0)).

3.5. Electrochemical oxidation for phenol

To evaluate the electrochemical degradation activity of the PbO_2-PVDF electrodes, phenol was chosen as the model pollutant for electrochemical oxidation in 0.1 mol L^{-1} Na_2SO_4 solution. The phenol removal efficiency and COD removal efficiency were shown in Fig. 7. From this figure, we could see that the phenol removal efficiency and COD removal efficiency increased after introducing the PVDF composites. And the PbO_2-PVDF(2.0) electrode exhibited the best performance for phenol degradation. The phenol removal efficiency and COD removal efficiency could reach to 99.9% and 87.2%, which were higher than that (81.5% and 63.9%) of PbO_2 electrode after 5 h electrolysis. After the dynamic fitting, we found that the degradation reaction followed pseudo-first-order kinetics and the kinetic constants (k) were listed in Table 1. From Table 1, it could be found that he maximum values of k were obtained at PbO_2-PVDF(2.0) electrode. The k values was 0.67 h^{-1} at PbO_2-PVDF(2.0) electrode, which was higher than that (0.31 h^{-1}) of PbO_2 electrode. In addition, the $t_{1/2}$ values for the degradation of phenol remarkably decreased from 2.55 h to 1.46 h, while the PbO_2-PVDF(2.0) electrode also showed a higher ICE and lower E_p than those of the other PbO_2-PVDF electrodes. The higher phenol removal rate for PbO_2-PVDF(2.0) electrode could be ascribed to the superhydrophobicity, higher OEP and higher active surface area. An electrode with super-

Table 1
The kinetics for the electrochemical degradation of phenol (electrolysis time: 5 h).

Electrode	Rate constants (k, h^{-1})[a]	Half-lives ($t_{1/2}$, h)	R^2	ICE (%)[b]	E_p (kWh $gCOD^{-1}$)[c]
PbO_2	0.31	2.55	0.991	5.6	0.493
PbO_2-PVDF(0.1)	0.37	2.24	0.988	6.8	0.406
PbO_2-PVDF(0.25)	0.44	2.02	0.988	7.0	0.391
PbO_2-PVDF(0.5)	0.49	1.87	0.989	7.6	0.362
PbO_2-PVDF(1.0)	0.58	1.65	0.990	8.6	0.319
PbO_2-PVDF(2.0)	0.67	1.46	0.988	10.0	0.275

[a] Pseudo-first-order rate constant of electrochemical degradation.
[b] The values of ICE and E_p were both obtained at the time of 50% COD removal.
[c] The values of ICE and E_p were both obtained at the time of 50% COD removal.

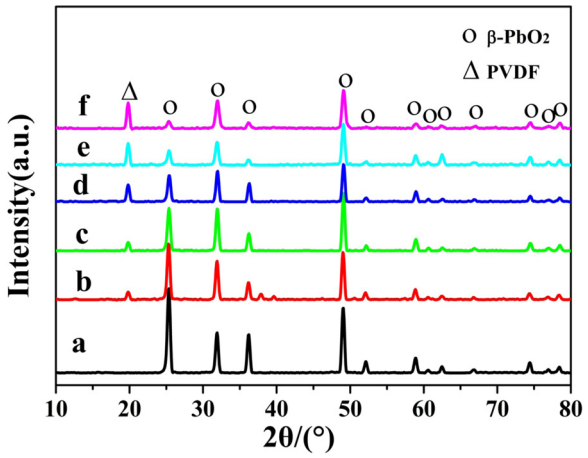

Fig. 4. XRD patterns of the different PbO_2-PVDF electrodes (a: PbO_2, b: PbO_2-PVDF(0.1), c: PbO_2-PVDF(0.25), d: PbO_2-PVDF(0.5), e: PbO_2-PVDF(1.0), f: PbO_2-PVDF(2.0)).

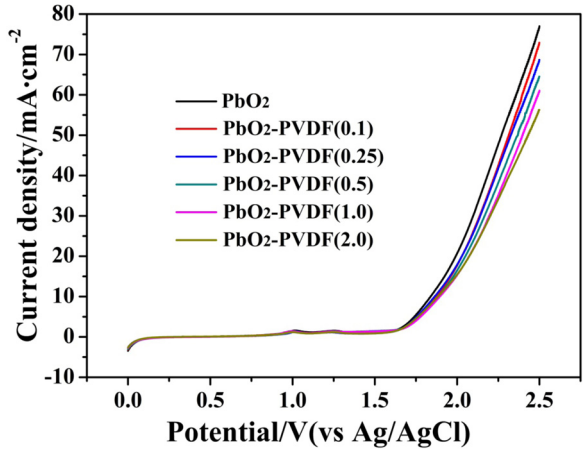

Fig. 5. Linear sweep voltammetric curves of PbO_2-PVDF electrodes in 0.5 mol L^{-1} Na_2SO_4 solution, scan rate: 50 mV s^{-1}.

hydrophobic surface could lower the adsorption capacity for HO•, generate more free HO• radicals and increase the utilization of HO• radicals. Meanwhile, the higher OEP and higher active surface area could also prohibit the evolution of oxygen, decrease E_p and generate more HO• radicals. To sum up the reasons, the PbO_2-PVDF(2.0) electrode showed the best performance for phenol degradation.

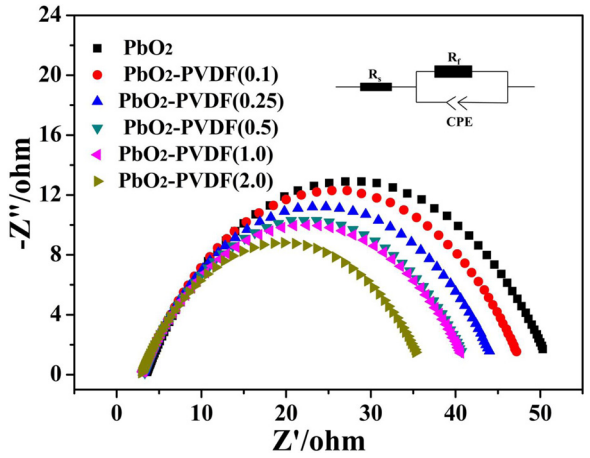

Fig. 6. Nyquist plots of PbO_2-PVDF electrodes and equivalent circuit model (the inset) in 0.5 mol L^{-1} Na_2SO_4 solution.

3.6. Generation capacity of HO• radicals and XPS analysis

In order to compare the ability for HO• generated on the selected electrodes. The concentration of HO• after electrolysis for 0.5 h and 1 h at 50 mA cm^{-2} are determined quantitatively (Fig. 8). From Fig. 8, it could be seen that the concentration of HO· increased with the increase of the PVDF doping amount. The PbO_2-PVDF(2.0) electrode showed strongest capacity for HO• generation. The HO• concentrations of PbO_2-PVDF(2.0) electrode were 7.19 μM and 14.17 μM after electrolysis for 0.5 h and 1 h, which was higher than that (4.61 μM and 8.39 μM) of PbO_2 electrode. A large number of HO• radicals could greatly promote the degradation of organic compounds. Therefore, this result was consistent with the results of the removals effectiveness of phenol and COD.

To further analyzed the reason for the enhancement of electrocatalytic activity of PbO_2-PVDF(2.0) electrode, the XPS measurement was also tested for PbO_2 electrode and PbO_2-PVDF(2.0) electrode (Fig. 9). The XPS data of chemical states of O on the electrode surface is shown in Table 2. Fig. 9a exhibits the survey spectra of PbO_2 electrode and PbO_2-PVDF(2.0) electrode, from which it could be clearly observed that the peaks of Pb and O existed in sample PbO_2 electrode. In addition, the F was also detected in the

Table 2
XPS data of chemical states of O on the electrode surface.

Electrode	Binding energy (eV) O1s (O_L)	O1s (O_{ad})	ε% $O_{ad}/(O_{ad}+O_L)$100%	η (O_{ad}/O_L)
PbO_2	529.07	531.67	66.23	1.96
PbO_2-PVDF(2.0)	529.17	531.17	88.59	7.76

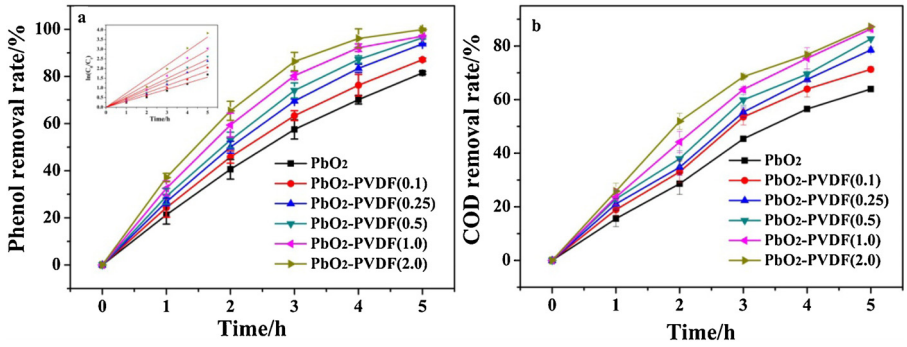

Fig. 7. Performance of the PbO_2-PVDF electrodes for phenol degradation. (a) phenol removal efficiency and (b) COD removal efficiency.

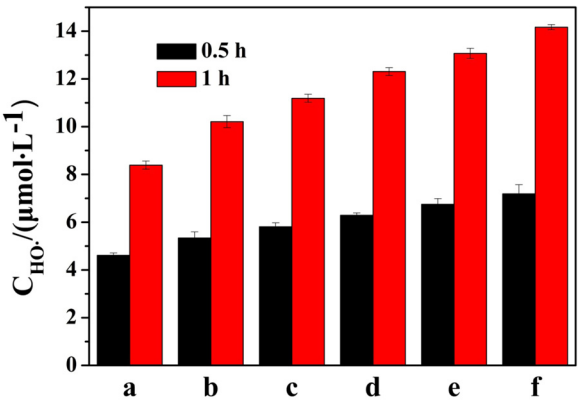

Fig. 8. Concentration evolution of HO· radicals on the different PbO_2-PVDF electrodes after electrolysis for 0.5 h and 1 h in 0.1 mol L^{-1} Na_2SO_4 solution (a: PbO_2, b: PbO_2-PVDF(0.1), c: PbO_2-PVDF(0.25), d: PbO_2-PVDF(0.5), e: PbO_2-PVDF(1.0), f: PbO_2-PVDF(2.0)).

PbO_2-PVDF(2.0) electrode surface except for Pb and O, indicating the PVDF was successfully doped into the PbO_2 electrode. Fig. 9b showed the core level F1s spectrum for PbO_2-PVDF(2.0) electrode. The binding energies of F 1s peaks at 688.15 eV was consistent with (-CH_2-CF_2-)n, which also proved the existence of PVDF composites. Fig. 9c and d showed the core level O1s spectra of PbO_2 electrode and PbO_2-PVDF(2.0) electrode. As shown in Fig. 9c, there exist two forms of oxygen in the electrode coating. The one at around 529 eV was assigned to strongly bounded lattice oxygen (O_L), while the peak at around 531 eV was attributed to adsorbed hydroxyl oxygen (O_{ad}) [37]. As shown in Table 2, it could be seen that the proportion (ε) of O_{ad} for PbO_2-PVDF(2.0) electrode was 88.59%, which was higher than that (66.23%) for PbO_2 electrode. It was widely accepted that the O_{ad} is related to active oxygen species (HO•). Therefore, the higher O_{ad} proportion mean that more HO• free radicals would be generated, which also account for the best performance for phenol degradation in this study [38].

3.7. Safety evaluation of PbO_2-PVDF electrodes

The leakage of Pb element in the electrolysis process was a main drawback of PbO_2 electrode [3,39]. It may cause a potential risk for large scale applications of the electrochemical technology. Therefore, the concentration of leached Pb in the electrolyte during the process of electrochemical oxidation was analyzed by

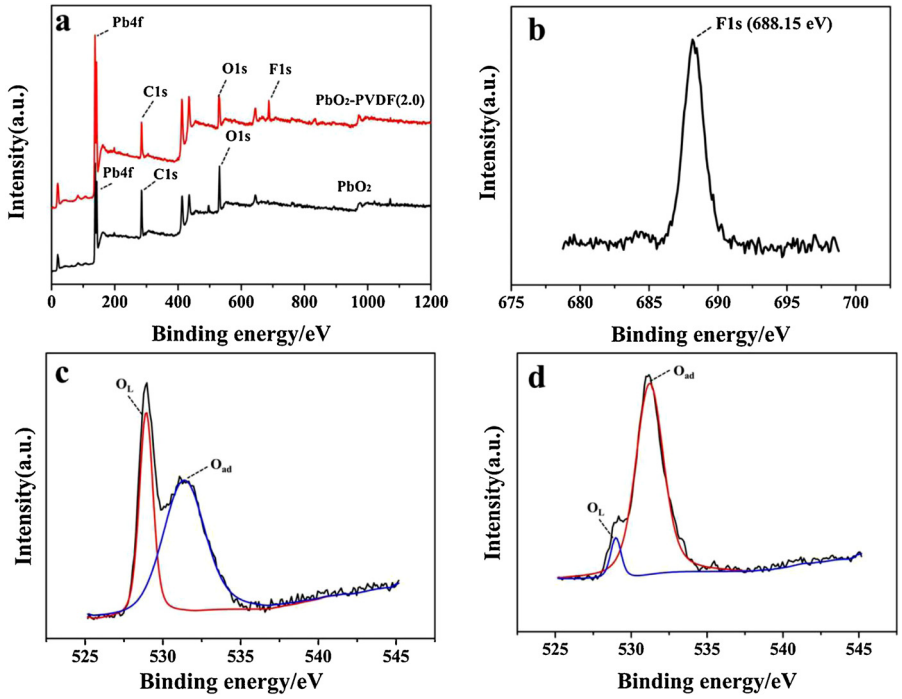

Fig. 9. XPS spectra of metal elements in PbO_2 electrode and PbO_2-PVDF(2.0) electrode. (a) XPS fully scanned spectra; (b) F 1s core level spectrum; (c) O 1s core level spectrum for PbO_2 electrode; (d) O 1s core level spectrum for PbO_2-PVDF(2.0) electrode.

inductively coupled plasma atomic emission spectroscopy (ICP-AES). To evaluate the safety of the PbO_2-PVDF electrodes, the concentration of Pb elements released from the electrodes after 120 min electrolysis in 0.1 mol L^{-1} Na_2SO_4 solution (50 mA cm^{-2}) were determined (Table S4). For PbO_2 electrode, the concentration of leached Pb was 0.027 mg L^{-1}. After PVDF doping, the concentration of Pb leakage decreased significantly. The lowest concentration of Pb (0.0041 mg L^{-1}) was obtained at PbO_2-PVDF(2.0) electrode, which was below the drinking water ordinance limits (GB5749-2006, Pb < 0.01 mg L^{-1}). Therefore, we could conclude that PVDF doping could significantly inhibit the anodic dissolution of the PbO_2 coating and improve the safety of the PbO_2 electrode.

3.8. Electrode stability evaluation

Electrode stability is also an important index to evaluate the electrode quality. Fig. 10 shows the time course of cell potential in the accelerated life test for different PbO_2-PVDF electrodes. The electrodes all experienced a stable stage before the cell potential of around 4.5 V, and then the cell potential increased sharply. According to Fig. 10, it could be evidently observed that after PVDF doping, the stability of the electrode were obviously improved. The longest accelerated service lifetime was obtained at PbO_2-PVDF(1.0) electrode (501 h), followed by PbO_2-PVDF(2.0) electrode (479 h), PbO_2-PVDF(0.5) electrode (386 h), PbO_2-PVDF(0.25) electrode (360.5 h), PbO_2-PVDF(0.1) electrode (306.5 h), which was all longer than that of PbO_2 electrode (118.5 h) (Table S2).

The reason for the accelerated service lifetime enhancement by PVDF doping could be explained as follows. Firstly, after PVDF modification, the surface of PbO_2-PVDF electrodes were more compact, integrity and the cracks on PbO_2 electrodes surface disappeared. Therefore, the electrolyte was difficult to penetrate coating through cracks and pores. In addition, the compact surface could also inhibit the coating flake caused by the internal O_2 evolution [40]. Secondly, after the addition of PVDF composites, the hydrophobicity of the electrodes were improved. Meanwhile, PVDF composites could also convert the activated substrates to hydroxyl radical in adsorbed state and restrain the movement and expansion of the free oxygen atoms to the electrode interior. Therefore, more HO• radicals were separated from the surface coating and diffused into the aqueous solution, which greatly inhibited the erosion of the active species (HO• radicals) on the coating. Thirdly, the F element existed in PVDF composites. It was known to all, the F^- ions doping could decreased the diffusion of oxygen atoms towards the Ti substrate, weaken the major side reaction of oxygen evolution, improve the defense ability and the binding force between the substrate and PbO_2 coatings, which also resulted in the enhancement of accelerated service lifetime [28,41–43]. Besides, many researchers have also reported that the doping of F can prolong the electrode service life and improve the electrode stability [44–46]. However, the excessive F doping may lead to the decrease of electrode service life. Therefore, when the doping amount of PVDF was higher than 1 g L^{-1}, the accelerated service lifetime decreased slightly. Consequently, 1 g L^{-1} PVDF was considered as the most suitable doping amount to improve stability in this study.

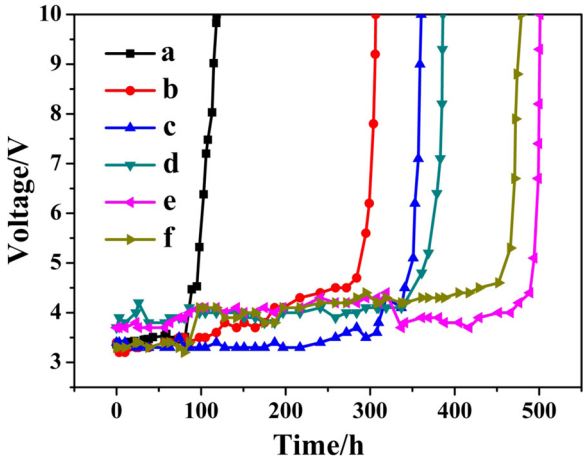

Fig. 10. Accelerated life test of PbO_2-PVDF electrodes in 3 mol L^{-1} H_2SO_4 solution at current density of 500 mA cm^{-2} (a: PbO_2, b: PbO_2-PVDF(0.1), c: PbO_2-PVDF(0.25), d: PbO_2-PVDF(0.5), e: PbO_2-PVDF(1.0), f: PbO_2-PVDF(2.0)).

4. Conclusions

A novel PbO_2 electrode with a high oxygen evolution potential (OEP) and long service life was modified by PVDF composites through co-deposition method and used for electrochemical degradation of phenol. PVDF modification could improve the film morphology, increase OEP and reduce the electrode film impedance. During the electrochemical oxidation process, the electrochemical oxidation of phenol followed pseudo-first-order kinetics and the PbO_2-PVDF(2.0) electrode showed the best performance on degradation of phenol. The k values was 0.67 h^{-1} at PbO_2-PVDF(2.0) electrode, which was higher than that 0.31 h^{-1} of PbO_2 electrode. The PbO_2-PVDF(2.0) electrode also showed a higher ICE and lower E_p than that of the other PbO_2-PVDF electrodes. In addition, the results of HO• radicals detection and XPS test showed that the PbO_2-PVDF(2.0) electrode showed strongest capability for HO• generation and the proportion of adsorbed hydroxyl oxygen (O_{ad}) for PbO_2-PVDF(2.0) electrode was 88.59%, which was higher than that (66.23%) for PbO_2 electrode. Furthermore, PVDF modification could greatly improved the stability of the electrodes. PbO_2-PVDF(1.0) electrode showed the longest service life (501 h), which was more than 4 times longer than PbO_2 electrode (118.5 h). In summary, considering the electrodecatalytic performance and stability of the electrodes, the optimum doping amount of PVDF obtained for electrochemical deposition was between 1 g L^{-1}–2 g L^{-1} in this study.

Acknowledgement

This work was supported by the National Natural Science Foundation of China (Grant No. 21507104).

Appendix A. Supplementary data

Supplementary data associated with this article can be found, in the online version, at http://dx.doi.org/10.1016/j.apsusc.2016.07.123.

References

[1] E. Brillas, C.A. Martínez-Huitle, Decontamination of wastewaters containing synthetic organic dyes by electrochemical methods. An updated review, Appl. Catal. B: Environ. 166–167 (2015) 603–643.
[2] C.A. Martinez-Huitle, S. Ferro, Electrochemical oxidation of organic pollutants for the wastewater treatment: direct and indirect processes, Chem. Soc. Rev. 35 (2006) 1324–1340.
[3] J. Chen, Y. Xia, Q. Dai, Electrochemical degradation of chloramphenicol with a novel Al doped PbO2 electrode: performance, kinetics and degradation mechanism, Electrochim. Acta 165 (2015) 277–287.
[4] Y.H. Cui, X.Y. Li, G. Chen, Electrochemical degradation of bisphenol A on different anodes, Water Res. 43 (2009) 1968–1976.
[5] G. Zhao, Y. Zhang, Y. Lei, B. Lv, J. Gao, Y. Zhang, D. Li, Fabrication and electrochemical treatment application of a novel lead dioxide anode withSuperhydrophobic surfaces high oxygen evolution potential, and oxidation capability, Environ. Sci. Technol. 44 (2014) 1754–1759.
[6] B. Cercado-Quezada, M.-L. Delia, A. Bergel, Electrochemical micro-structuring of graphite felt electrodes for accelerated formation of electroactive biofilms on microbial anodes, Electrochem. Commun. 13 (2011) 440–443.

[7] M.G. Tavares, L.V.A. da Silva, A.M. Sales Solano, J. Tonholo, C.A. Martínez-Huitle, C.L.P.S. Zanta, Electrochemical oxidation of methyl red using Ti/Ru0.3Ti0.7O2 and Ti/Pt anodes, Chem. Eng. J. 204–206 (2012) 141–150.
[8] L.S. Andrade, T.T. Tasso, D.L. da Silva, R.C. Rocha-Filho, N. Bocchi, S.R. Biaggio, On the performances of lead dioxide and boron-doped diamond electrodes in the anodic oxidation of simulated wastewater containing the Reactive Orange 16 dye, Electrochim. Acta 54 (2009) 2024–2030.
[9] M. Li, C. Feng, W. Hu, Z. Zhang, N. Sugiura, Electrochemical degradation of phenol using electrodes of Ti/RuO2-Pt and Ti/IrO2-Pt, J. Hazard. Mater. 162 (2009) 455–462.
[10] J.L. Fernaíndez, M.R.G.d. Chialvo, A.C. Chialvo, Kinetic study of the chlorine electrode reaction on Ti/RuO2 through the polarisation resistance part III: proposal of a reaction mechanism, Electrochim. Acta 47 (2002) 1145–1152.
[11] H. Lin, J. Niu, S. Ding, L. Zhang, Electrochemical degradation of perfluorooctanoic acid (PFOA) by Ti/SnO2-Sb, Ti/SnO2-Sb/PbO2 and Ti/SnO2-Sb/MnO2 anodes, Water Res. 46 (2012) 2281–2289.
[12] L. Xu, M. Li, W. Xu, Preparation and characterization of Ti/SnO2-Sb electrode with copper nanorods for AR 73 removal, Electrochim. Acta 166 (2015) 64–72.
[13] W. Zhang, H. Lin, H. Kong, H. Lu, Z. Yang, T. Liu, Preparation and characterization of lead dioxide electrode with three-dimensional porous titanium substrate for electrochemical energy storage, Electrochim. Acta 139 (2014) 209–216.
[14] G. Darabizad, M.S. Rahmanifar, M.F. Mousavi, A. Pendashteh, Electrodeposition of morphology- and size-tuned PbO2 nanostructures in the presence of PVP and their electrochemical studies, Mater. Chem. Phys. 156 (2015) 121–128.
[15] X. Hao, Y. Quansheng, S. Dan, Y. Honghui, L. Jidong, F. Jiangtao, Y. Wei, Fabrication and characterization of PbO2 electrode modified with [Fe(CN)6]3- and its application on electrochemical degradation of alkali lignin, J. Hazard. Mater. 286 (2015) 509–516.
[16] A.Y. Bagastyo, J. Radjenovic, Y. Mu, R.A. Rozendal, D.J. Batstone, K. Rabaey, Electrochemical oxidation of reverse osmosis concentrate on mixed metal oxide (MMO) titanium coated electrodes, Water Res. 45 (2011) 4951–4959.
[17] H. An, H. Cui, W. Zhang, J. Zhai, Y. Qian, X. Xie, Q. Li, Fabrication and electrochemical treatment application of a microstructured TiO2-NTs/Sb–SnO2/PbO2 anode in the degradation of C.I. Reactive Blue 194 (RB 194), Chem. Eng. J. 209 (2012) 86–93.
[18] D. Shao, J. Liang, X. Cui, H. Xu, W. Yan, Electrochemical oxidation of lignin by two typical electrodes: ti/SbSnO2 and Ti/PbO2, Chem. Eng. J. 244 (2014) 288–295.
[19] X. Li, D. Shao, H. Xu, W. Lv, W. Yan, Fabrication of a stable Ti/TiOxHy/Sb-SnO2 anode for aniline degradation in different electrolytes, Chem. Eng. J. 285 (2016) 1–10.
[20] W. Zhang, H. Kong, H. Lin, H. Lu, W. Huang, J. Yin, Z. Lin, J. Bao, Fabrication, characterization and electrocatalytic application of a lead dioxide electrode with porous titanium substrate, J. Alloys Compd. 650 (2015) 705–711.
[21] H. Kong, W. Huang, H. Lin, H. Lu, W. Zhang, Effect of SnO2-Sb2O5 interlayer on electrochemical performances of a Ti-substrate lead dioxide electrode, Chin. J. Chem. 30 (2012) 2059–2065.
[22] D. Devilliers, E. Mahé, Modified titanium electrodes: application to Ti/TiO2/PbO2 dimensionally stable anodes, Electrochim. Acta 55 (2010) 8207–8214.
[23] X. Hao, S. Dan, Z. Qian, Y. Honghui, W. Yan, Preparation and characterization of PbO2 electrodes from electro-deposition solutions with different copper concentration, RSC Adv. 4 (2014) 25011.
[24] H. Kong, W. Li, H. Lin, Z. Shi, H. Lu, Y. Dan, W. Huang, Influence of F-doping on the microstructure, surface morphology and electrochemical properties of the lead dioxide electrode, Surf. Interface Anal. 45 (2013) 715–721.
[25] Q. Li, Q. Zhang, H. Cui, L. Ding, Z. Wei, J. Zhai, Fabrication of cerium-doped lead dioxide anode with improved electrocatalytic activity and its application for removal of rhodamine B, Chem. Eng. J. 228 (2013) 806–814.
[26] Y. Jin, F. Wang, M. Xu, Y. Hun, W. Fang, Y. Wei, C. Zhu, Preparation and characterization of Ce and PVP co-doped PbO2 electrode for waste water treatment, J. Taiwan Inst. Chem. Eng. 51 (2015) 135–142.
[27] B.J. Hwang, K.L. Lee, Electrocatalytic oxidation of 2-chlorophenol on a composite PbO2/polypyrrole electrode in aqueous solution, J. Appl. Electrochem. 26 (1996) 153–159.
[28] Z. Minghua, D. Qizhou, L. Lecheng, M. Chunan, W. Dahui, Long life modified lead dioxide anode for organic wastewater treatment:Electrochemical characteristics and degradation mechanism, Environ. Sci. Technol. 39 (2005) 363–370.
[29] Q. Dai, H. Shen, Y. Xia, F. Chen, J. Wang, J. Chen, The application of a novel Ti/SnO2–Sb2O3/PTFE-La-Ce-β-PbO2 anode on the degradation of cationic gold yellow X-GL in sono-electrochemical oxidation system, Sep. Purif. Technol. 104 (2013) 9–16.
[30] L.L. Sun, B. Li, Z.G. Zhang, W.H. Zhong, Achieving very high fraction of β-crystal PVDF and PVDF/CNF composites and their effect on AC conductivity and microstructure through a stretching process, Eur. Polym. J. 46 (2010) 2112–2119.
[31] A.K. Gupta, R. Bajpai, J.M. Keller, Morphological, crystallization and plasticization studies on isomorphic blends of poly (vinyl fluoride) (PVF) and poly (vinylidene difluoride) (PVDF): using microhardness, XRD and SEM techniques, J. Mater. Sci. 41 (2006) 5857–5861.
[32] M. Wang, J.-H. Shi, K.P. Pramoda, S.H. Goh, Microstructure, crystallization and dynamic mechanical behaviour of poly(vinylidene fluoride) composites containing poly(methyl methacrylate)-grafted multiwalled carbon nanotubes, Nanotechnology 18 (2007) 235701.
[33] C. Tai, J.-F. Peng, J.-F. Liu, G.-B. Jiang, H. Zou, Determination of hydroxyl radicals in advanced oxidation processes with dimethyl sulfoxide trapping and liquid chromatography, Anal. Chim. Acta 527 (2004) 73–80.
[34] Y. Chen, L. Hong, H. Xue, W. Han, L. Wang, X. Sun, J. Li, Preparation and characterization of TiO2-NTs/SnO2-Sb electrodes by electrodeposition, J. Electroanal. Chem. 648 (2010) 119–127.
[35] L. Zhang, L. Xu, J. He, J. Zhang, Preparation of Ti/SnO2-Sb electrodes modified by carbon nanotube for anodic oxidation of dye wastewater and combination with nanofiltration, Electrochim. Acta 117 (2014) 192–201.
[36] D. Shao, W. Yan, X. Li, H. Xu, Fe3O4/Sb–SnO2 granules loaded on Ti/Sb–SnO2 electrode shell by magnetic force: good recyclability and high electro-oxidation performance, ACS Sustain. Chem. Eng. 3 (2015) 1777–1785.
[37] Y. Duan, Q. Wen, Y. Chen, T. Duan, Y. Zhou, Preparation and characterization of TiN-doped Ti/SnO2-Sb electrode by dip coating for Orange II decolorization, Appl. Surf. Sci. 320 (2014) 746–755.
[38] S. Yang, Y. Feng, J. Wan, W. Zhu, Z. Jiang, Effect of CeO2 addition on the structure and activity of RuO2/γ-Al2O3 catalyst, Appl. Surf. Sci. 246 (2005) 222–228.
[39] J. Niu, H. Lin, J. Xu, H. Wu, Y. Li, Electrochemical mineralization of perfluorocarboxylic acids (PFCAs) by ce-doped modified porous nanocrystalline PbO2 film electrode, Environ. Sci. Technol. 46 (2012) 10191–10198.
[40] Y. Yao, C. Zhao, J. Zhu, Preparation and characterization of PbO2–ZrO2 nanocomposite electrodes, Electrochim. Acta 69 (2012) 146–151.
[41] F.L. Souza, J.M. Aquino, K. Irikura, D.W. Miwa, M.A. Rodrigo, A.J. Motheo, Electrochemical degradation of the dimethyl phthalate ester on a fluoride-doped Ti/beta-PbO2 anode, Chemosphere 109 (2014) 187–194.
[42] A.B. Velichenko, D. Devilliers, Electrodeposition of fluorine-doped lead dioxide, J. Fluorine Chem. 128 (2007) 269–276.
[43] A.B. Velichenko, D.V. Girenko, S.V. Kovalyov, A.N. Gnatenko, R. Amadelli, F.I. Danilov, Lead dioxide electrodeposition and its application: influence of fluoride and iron ions, J. Electroanal. Chem. 454 (1998) 203–208.
[44] L.S. Andrade, R.C. Rocha-Filho, N. Bocchi, S.R. Biaggio, J. Iniesta, V. Garcia-Garcia, V. Montiel, Degradation of phenol using Co- and Co, F-doped PbO(2) anodes in electrochemical filter-press cells, J. Hazard. Mater. 153 (2008) 252–260.
[45] Q. Qiao, L. Wang, J. Sh, J. Jin, Y. Li, Properties of fluoride-doped β-PbO2 electrodes and their electrocatalytic activities in degradation of acid orange II, Int. J. Electrochem. Sci. 10 (2015) 10639–10650.
[46] J. Cao, H. Zhao, F. Cao, J. Zhang, The influence of F- doping on the activity of PbO2 film electrodes in oxygen evolution reaction, Electrochim. Acta 52 (2007) 7870–7876.